Zuerst ersch. in : Cell Calcium ; 53 (2013), 3. - S. 204-216
http://dx.doi.org/10.1016/j.ceca.2012.11.016

A set of SNARE proteins in the contractile vacuole complex of *Paramecium* regulates cellular calcium tolerance and also contributes to organelle biogenesis

Barbara Schönemann, Alexander Bledowski, Ivonne M. Sehring[1], Helmut Plattner*

Department of Biology, University of Konstanz, 78457 Konstanz, Germany

A B S T R A C T

The contractile vacuole complex (CVC) of freshwater protists serves the extrusion of water and ions, including Ca^{2+}. No vesicle trafficking based on SNAREs has been detected so far in any CVC. SNAREs (soluble NSF [N-ethylmaleimide sensitive factor] attachment protein receptors) are required for membrane-to-membrane interaction, i.e. docking and fusion also in *Paramecium*. We have identified three v-/R- and three t/Q-SNAREs selectively in the CVC. Posttranscriptional silencing of Syb2, Syb6 or Syx2 slows down the pumping cycle; silencing of the latter two also causes vacuole swelling. Increase in extracellular Ca^{2+} after Syb2, Syb6 or Syx2 silencing causes further swelling of the contractile vacuole and deceleration of its pulsation. Silencing of Syx14 or Syx15 entails lethality in the Ca^{2+} stress test. Thus, the effects of silencing strictly depend on the type of the silenced SNARE and on the concentration of Ca^{2+} in the medium. This shows the importance of organelle-resident SNARE functions (which may encompass the vesicular delivery of other organelle-resident proteins) for Ca^{2+} tolerance. A similar principle may be applicable also to the CVC in widely different unicellular organisms. In addition, in *Paramecium*, silencing particularly of Syx6 causes aberrant positioning of the CVC during de novo biogenesis before cytokinesis.

Keywords:
Ca^{2+}
Calcium
Ciliate
Contractile vacuole
Membrane traffic
Osmoregulation
Paramecium
SNARE

1. Introduction

To survive in their hypotonic ambient medium, freshwater organisms such as protozoa as well as some other lower eukaryotes have to permanently cope with the leakage of water. In evolution many of these organisms have acquired a contractile vacuole (CV) complex (CVC) which collects the excess of water for periodic expulsion by exocytosis [1]. This is also true of ciliates, such as *Paramecium* [2,3] and *Tetrahymena* [4]. Other examples are amoebozoa such as *Amoeba proteus* [5] and *Dictyostelium discoideum* [6,7], different algae [8] including the flagellate *Chlamydomonas* [9], as well as *Trypanosoma cruzi* [10]. A large number of proteins – except SNAREs – has been detected in the CVC particularly of *D. discoideum* [11] and *T. cruzi* [12].

A salient feature of CVC function is the occurrence of a H^+-ATPase (=H^+-pump or V-ATPase) in widely different cell types [12]. This includes *A. proteus* [13], *Dictyostelium* [6,14] and *Paramecium* [15–18]. Clarke et al. [19] proposed that fluid accumulation for extrusion by the CV is driven by this pump. This multimeric protein complex encompasses a transmembrane V0 and a catalytic head/V1 complex. As shown first with *Paramecium*, the electrogenic generation of a H^+-gradient attracts water chemiosmotically from the cytosol, the CV swells until it discharges water, Ca^{2+} and other ions [20–22], by exocytotic fusion with the cell membrane at the porus [3] whose location is epigenetically determined [23]. In *Paramecium* there occurs some sub-compartmentation within the CVC [3]: as seen in the light microscope (LM) the CV is connected to radial arms (=collecting canals) via ampullae. In a more distal region radial arms are continuous with a great number of tightly packed tubules, the spongiome. This consists of branching interconnected smooth membranes (smooth spongiome) which, in more distal parts, are continuous with the decorated spongiome. In the electron microscope (EM) this part looks decorated as it is studded with ~15 nm large pegs [24]. These represent the multimeric V1 head parts of the H^+-ATPase [15,16] of which a number of subunits (SUs) have been identified [17,18].

Though CVCs clearly serve the expulsion of an excess of Ca^{2+} and other ions in *Paramecium* [21,22] molecular details or the function of the CVC emerge only slowly. Extrusion of Ca^{2+} is even more important as $^{45}Ca^{2+}$ flux, measured in unstimulated *Paramecium* cells, is very strong [25]. Sequestration of Ca^{2+}, powered by the ΔH^+ between the cytosol and the CVC lumen [21,22], probably involves antiporter systems. Although not identified as yet, candidates are known from the genome of widely different protozoa [26] including *Dictyostelium* (probably in their CVC [27]), and *Paramecium* (unpubl. data). Furthermore, in *Paramecium* inositol

* Corresponding author. Tel.: +49 7531 88 2228; fax: +49 7531 88 2245.
E-mail address: helmut.plattner@uni-konstanz.de (H. Plattner).
[1] Present address: Sars International Centre for Marine Molecular Biology, Universitetet i Bergen, Norway.

1,4,5-trisphosphate receptors (IP_3Rs) are contained in the smooth membranes of the CVC where they are constitutively active and allow for some fine-tuning by reflux of Ca^{2+} from the CVC into the cytosol [28]. Several additional Ca^{2+}-release channels (CRCs) occur in the CVC, their function also awaiting elucidation [29].

Microtubules expand over the entire CVC of *Paramecium*, from the porus, over CV and ampullae to the tips of the radial arms [30]. They form a scaffold during the transformation of the membranes accompanying a pulsation cycle, as described above [31]. Therefore, microtubules are also useful for localizing CVCs even in case of organelle obliteration under experimental conditions. No actin has ever been found in association with the CVC [32,33].

Additional components of the CVC of *Paramecium* include SNARE (soluble NSF [N-ethylmaleimide sensitive factor] attachment proteins [SNAP] receptor) proteins. These are known to mediate docking of homo- and heterotypic membranes in a cell and finally fusion [34]. They allow, e.g. fusion of a secretory vesicle with the cell membrane and, therefore, are grossly subdivided into vesicle- and target- (v-/t-) SNAREs or, according to the central amino acid in the zero-layer, as R- and Q-SNAREs [35]. v-/R- and t-/Q-SNARE interaction is mediated by the specific AAA-ATPase-type chaperone, NSF [36] which has also been identified in *Paramecium* [37]. We have identified a battery of SNAREs in *Paramecium* [38–43], also in its CVC (this paper). Small GTPases are additional components to be considered for vesicle trafficking [44], also in the CVC of *Tetrahymena* [45].

On the background of the CVC components currently known from *Paramecium*, we now try to find some basic clues to the relevance of SNAREs for organelle biogenesis and function, particularly for the regulation of Ca^{2+} homeostasis. Posttranslational gene silencing by feeding transformed bacteria [46], as established for, and routinely practiced with *Paramecium*, is combined with (ultra-)structural analysis and functional tests, such as tolerance to increased Ca^{2+} concentration in the medium, $[Ca^{2+}]_o$. Although molecular interactions are too complex to pinpoint any precise molecular mechanism for each aspect we can show that specific SNAREs are clearly involved in CVC formation and function in *Paramecium*, particularly with regard to Ca^{2+} tolerance.

2. Materials and methods

2.1. Cell cultures

We used the *Paramecium tetraurelia* wildtype strains 7S and d4-2, both derived from stock 51S [47]. Cells were cultivated in a decoction of dried lettuce, monoxenically inoculated with *Enterobacter aerogenes* and supplemented with 0.4 $\mu g\,ml^{-1}$ sitosterol, as indicated previously [32]. For the experiments described the cultivation medium was supplemented with 1 mM KCl and 1 mM $CaCl_2$ (increased to 5 mM in Ca^{2+} stress experiments).

2.2. Vectors used and gene silencing methodology

The NSF genes have been annotated previously by Kissmehl et al. [37], genes of the Syb2, Syb6 by Schilde et al. [38] and of Syb9 genes by Schilde et al. [40] and the Syx genes Syx2, Syx14 and Syx15 by Kissmehl et al. [41]. As specified in the respective references, sequences of the respective genes were cloned in a pPD vector. In our current analysis we included Syb2 and a Syb1-1/Syb2-2 tandem construct, Syb6 [38], Syb9 [40] as well as Syx2, Syx14 and Syx15 [41]. Other vectors contained sequences of a NSF gene or of a NSF-green fluorescent protein (GFP) construct (see below). The latter was cloned into the enhanced GFP expression plasmid pPXV [48] as indicated previously [40,41]. As specified in the work cited above, the products thus obtained were controlled by PCR.

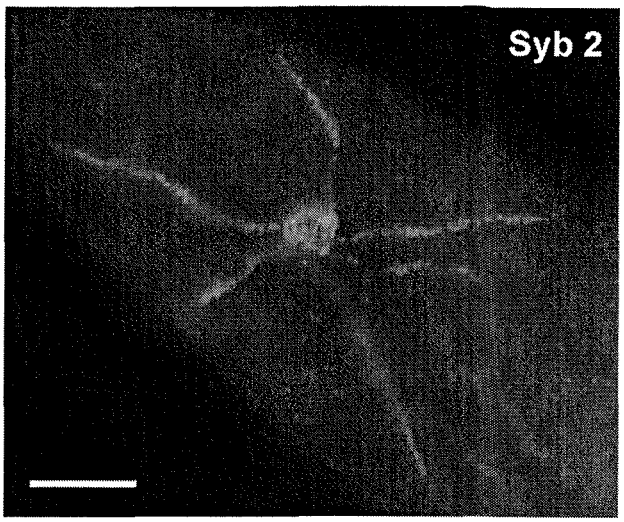

Fig. 1. Syb2 visualized as a carboxy-terminal GFP-fusion protein, as described by Schilde et al. [38]. Note punctate labeling over radial arms (or, according to Fig. 2, rather over the smooth spongiome) and the CV. Bar = 5 μm.

The NSF silencing construct was applied as described previously [37] and cells were grown for 36 h. Silencing constructs were used to transform *Escherichia coli* bacteria, RNase III-deficient strain HTT115, according to methods established by Timmons et al. [49], successfully adjusted to *Paramecium* by Galvani and Sperling [46] and applied by us for 65 h, as already in previous work with different SNAREs [38–41].

2.3. Antibody preparation

Antibodies (ABs) against Synaptobrevins used in this study have also been described previously in the context of our work with Syb2, Syb6 [38], Syb9 [40], and Syx2 [41]. We now included polyclonal ABs produced in rabbits against Syx14 and Syx15 using specific immunogenic sequences, i.e. ^{109}NRSNGGKQYKDTET^{122} for Syx14 and ^{102}KQEVAMQNLQRDD^{114} for Syx15. For any further details including affinity purification, see ref. [41]. Additional Western blots ascertained bands of correct molecular size (data not shown).

2.4. Fluorescence analyses

Cells have been prepared as indicated previously [38,40,41]. Briefly, cells were fixed in 4% formaldehyde in phosphate-buffered saline (PBS) with 1% Triton-X100 or 0.5% digitonin (Sigma, Taufkirchen, Germany) added, washed in PBS + 50 mM glycine and exposed to the respective ABs. Polyclonal ABs directed against the different SNAREs (see above) were counterstained with second AB conjugates type goat anti-rabbit coupled to Alexafluor^{488}, monoclonal ABs directed against tubulin with goat anti-mouse $F(ab)_2$ fragments coupled to Alexafluor^{594}. Fluorescent conjugates were from Molecular Probes (Eugene, OR). For conventional fluorescence microscopy and transmission mode imaging we used a Zeiss Axiovert 100TV equipped with the corresponding filter sets as described before [38,40,41]. Confocal images were obtained with a confocal laser-scanning LSM 510 microscope from Zeiss. Visualization of Syb2 as a GFP-fusion protein with GFP attached at the carboxy-terminal side was used here only exceptionally (Fig. 1). The procedure was as described before [40,41]. To control silencing of NSF we also have used a construct containing NSF sequences in tandem with a GFP sequence carboxy-terminally attached. We selected fluorescent cells for

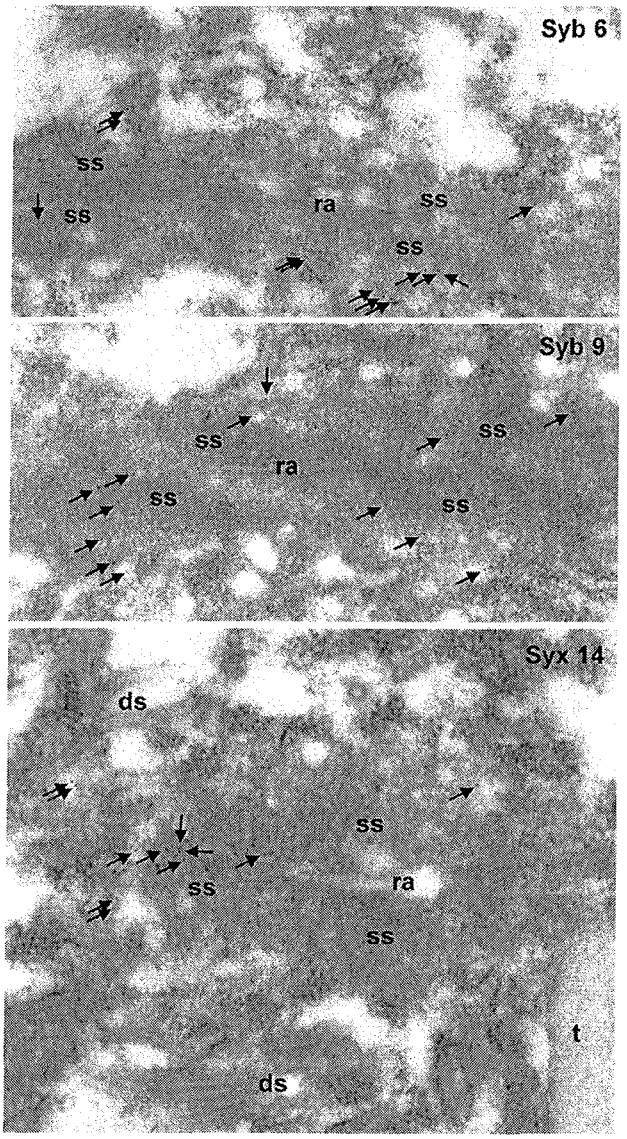

Fig. 2. Examples of immuno-gold EM localization (arrows) selectively in the smooth spongiome (ss), as shown for Syb6 (A), Syb9 (B) and Syx14 (C). Note that label also occurs in peripheral regions of the smooth spongiome, but not over the decorated spongiome (ds) and the radial arms (ra). t = trichocyst. Magnification 50,000×.

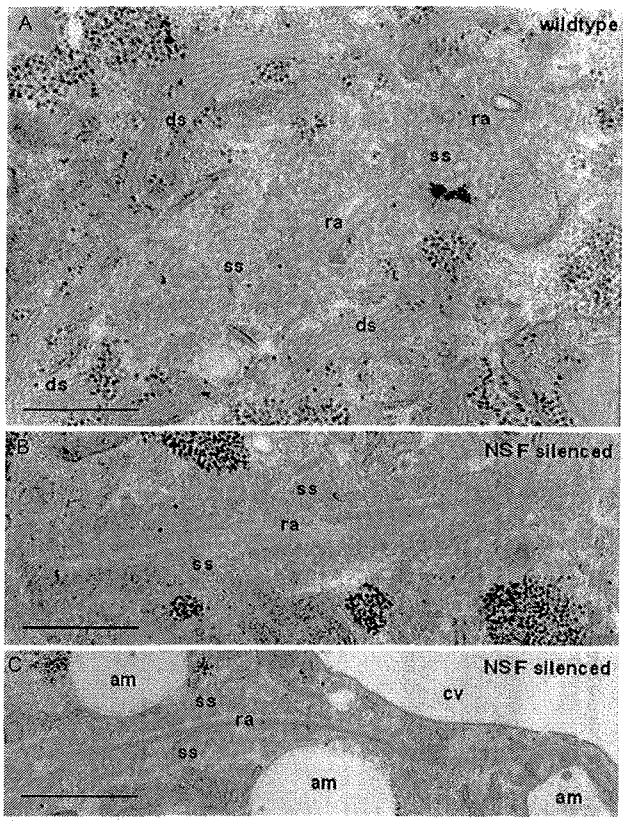

Fig. 3. Ultrastructural appearance of the CVC in a normal cell (A) and in cells silenced in NSF for 36 h as previously described [37] (B and C). Note in (A) the rich expression of the smooth spongiome (ss) around a radial arm (ra). The radial arm is cut in oblique orientation in the image center, and in cross-section in the top right part of the image. Note peripheral location of the decorated spongiome (ds). In (B) and (C) stages of spongiome obliteration are presented. Less in (B), but more in (C) the smooth spongiome is reduced, whereas no decorated spongiome is visible. In (C) one also recognizes the swollen contractile vacuole (cv) and ampullae (am). Bars = 0.5 μm.

epifluorescence microscopy in a Zeiss Axiovert 100TV equipped for GFP recording, to obtain clonal descendants for further analysis including electron microscopy (EM). All further methodical details including instrumentation have previously been published in more detail [38,40,41].

2.5. Analysis of structural and functional effects of SNARE silencing

Silencing of the different SNAREs has been extended to 65 h. (Cells mock-silenced with empty vector showed no changes.) Then a droplet with cells has been put, without medium change, on a glass slide, covered with paraffin oil to restrict motility. Under a stereomicroscope connected to a digital image recording unit cells have been video-recorded randomly for 3 min. Final evaluation of structural changes (swelling) of the CV at the light microscope (LM) level has been done only with situations where CVs and cell body were both found in a strictly median plane. Since in pilot experiments the anterior and posterior CV were of the same size and reacted equally to the different manipulations, we did not discriminate between the two. The area size of a CV at its maximal expansion and of the corresponding cell, both precisely in median plane but randomly taken from the recorded image collection of pumping cycles, was digitized and evaluated by Excel. From these data we then have calculated the size of the CV relative to the entire cell. (In pilot evaluation series we had seen that this procedure is most appropriate to describe phenomena such as organelle swelling, although tendencies were the same with absolute values of CV size.) In addition we have determined the duration of the contraction cycle under the same conditions. For statistical evaluation we determined p-values by Student's t-test and standard error of the mean (s.e.m.). For viability tests the number of cells was counted in several sample drops of defined size, each containing >100 cells.

The same parameters were also determined under Ca^{2+} stress as follows. With the cells still in the silencing medium, the Ca^{2+} concentration in the medium $[Ca^{2+}]_o$ was increased from 1 mM to 5 mM. In some controls we registered reversibility by reverting $[CaCl_2]_o$ to 1 mM. For further controls we applied $MgCl_2$, 2-deoxyglucose or L-lysine, all 5 mM in the presence of 1 mM $CaCl_2$, but none of these controls resulted in effects comparable to 5 mM $CaCl_2$ (see Section 3.4).

2.6. EM analysis of ultrastructure and immuno-EM analysis

For visualizing ultrastructural details cells have been routinely fixed in 5% glutaraldehyde, followed by 1% OsO_4, both in 0.1 M cacodylate buffer pH 7.2, dehydrated in acetone series and embedded in Spurr's epoxide resin. Ultrathin sections have been routinely stained with aqueous uranyl acetate and lead citrate pH 12.0.

For immuno-gold EM analysis we have used the same methods as indicated previously [29]. In brief, cells have been rapidly injected in a 0 °C fixative of 8% formaldehyde and 0.1% glutaraldehyde in Pipes buffer pH 7.2, washed with 50 mM glycine, dehydrated in increasing ethanol concentrations, and embedded in LR Gold resin (London Resin, London, UK) for UV polymerization at −35 °C. Ultrathin sections were incubated with ABs against a selection of SNAREs, followed by protein A–gold (5 nm) conjugates ($pA\text{–}Au_{5\,nm}$) obtained from the Cell Biology Center, University Medical Center Utrecht (NL). Controls incubated with pre-immune sera or with $pA\text{–}Au_{5\,nm}$ conjugate only routinely displayed a negligible amount of gold granules. Ultrathin sections have been analyzed in a Zeiss electron microscope, EM10, operated at 100 kV with a 30 μm objective aperture.

3. Results

3.1. Boundary conditions derived from previous work and from molecular biology data

Principally we aimed at manipulating CVC biogenesis and effects of Ca^{2+} stress (see Section 2). We started with the method elaborated by Iwamoto et al. [50] which enables the induction of supernumerary CVCs in a hypertonic medium with increased $[Ca^{2+}]_o$. Though well reproducible (data not shown) this method unfortunately turned out to be inefficient with cultures raised monoxenically before subsequent gene silencing by feeding transformed bacteria. Using throughout this study monoxenic cultures from the beginning, gene silencing was combined with immuno-localization. This gave important clues to steadily ongoing SNARE-mediated vesicle trafficking for "cryptic biogenesis", to its relevance for Ca^{2+} tolerance, and eventually to "overt biogenesis" when new CVCs are formed occasionally in some cells before cytokinesis.

We show examples of the normal localization of SNAREs in the CVC of normal cells at the LM and EM level (Figs. 1 and 2), followed by silencing of the SNARE chaperone, NSF, at the EM level (Fig. 3), AB-fluorescence analysis of cells silenced in individual CVC-resident SNAREs (Figs. 4 and 5) and ultrastructural changes due to silencing of one of the prominent CVC SNAREs (Fig. 6). Finally we document the effect of silencing of Syx6, on the positioning of newly forming CVCs (Fig. 7). Furthermore we tested the effect of silencing of individual CVC SNAREs on organelle performance and the effect of Ca^{2+} stress (Figs. 7 and 8).

Prerequisite to differential silencing is a difference in nucleotides at the mRNA level which should be about ≥15% [46]. This corollary is fulfilled. Comparing Syb2 with Syb6 and Syb 9 the difference is 71% and 70%, respectively, and comparing Syb6 and Syb9 it is 68%. (In each case subform-1 is compared, e.g. Syb2-1, etc.) For Syx2 in comparison to Syx14 and Syx 15 we determined a difference of 68% and 66%, respectively, for Syx14 and Syx15 60%. The differences between subforms-1 and -2, where available, is 19% for Syb2-1 and Syb2-2, 45% for Syb9-1 and Syb9-2, 10% for Syx2-1 and Syx2-2, 7% for Syx14-1 and Syx14-2. Thus, among SNAREs analyzed in more detail here, Syb2 is close to the limits, suggesting the requirement of differential silencing assays for the two ohnologs.

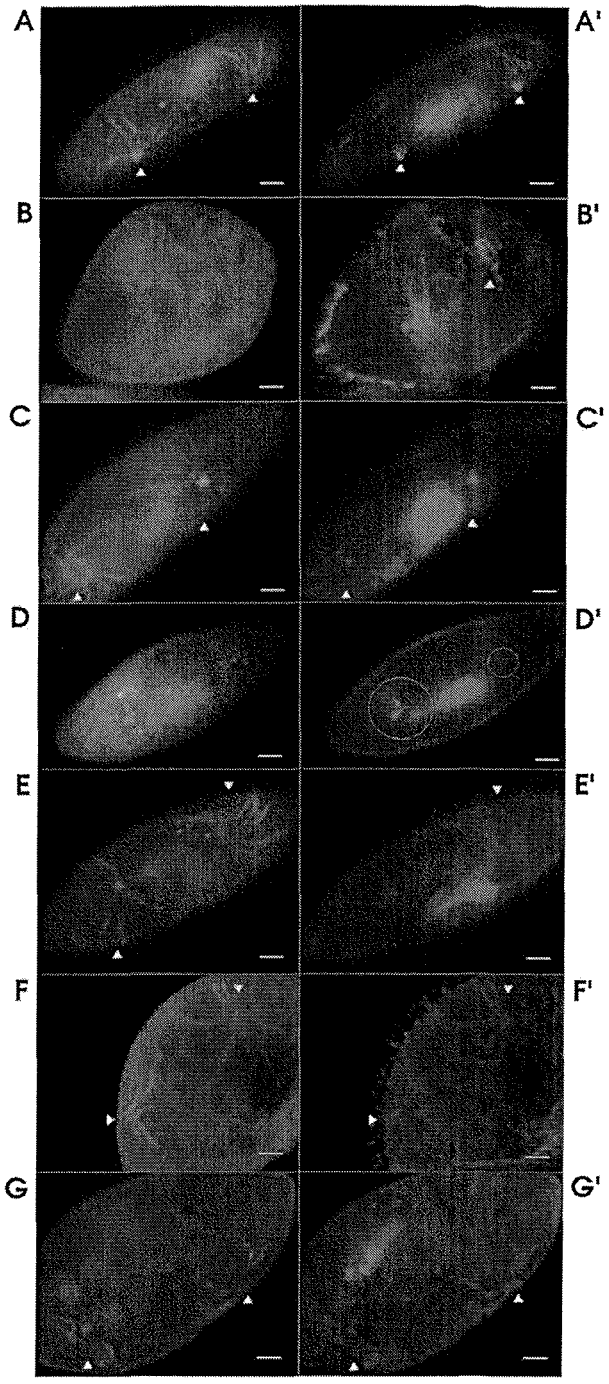

Fig. 4. Staining of the CVC by ABs against different SNAREs and other membrane components (A–G) and coordinated images representing staining with anti-tubulin ABs (A'–G'). Unless affected by gene silencing, the CVCs are clearly recognizable (by their radial arms emanating from a dot representing the contractile vacuole) after AB and tubulin staining, but AB staining may be faded in silenced cells (B and D). (A and A') staining for Syb2/tubulin in a normal cell, with the CVCs clearly visible. (B and B') Syb2 silencing makes the CVC invisible in anti-Syb2 AB staining. (C and C') normal cell with staining for Syx2/tubulin, with clearly recognizable CVCs. (D and D') Syx2 silencing makes the CVC barely recognizable by anti-Syx2 AB staining while tubulin staining occurs. (E and E') Syx2 silencing followed by staining for Syb2/tubulin. Note maintenance of the organelle integrity and of staining for the non-silenced SNARE, Syb2. (F and F') Syx2 silencing followed by staining for the a2 SU of the H^+-ATPase and tubulin which both are clearly visible. (G and G') Syx2 silencing followed by staining for the CVC-resident IP_3R and tubulin. Note persistence of labeling of both components. Bars = 10 μm.

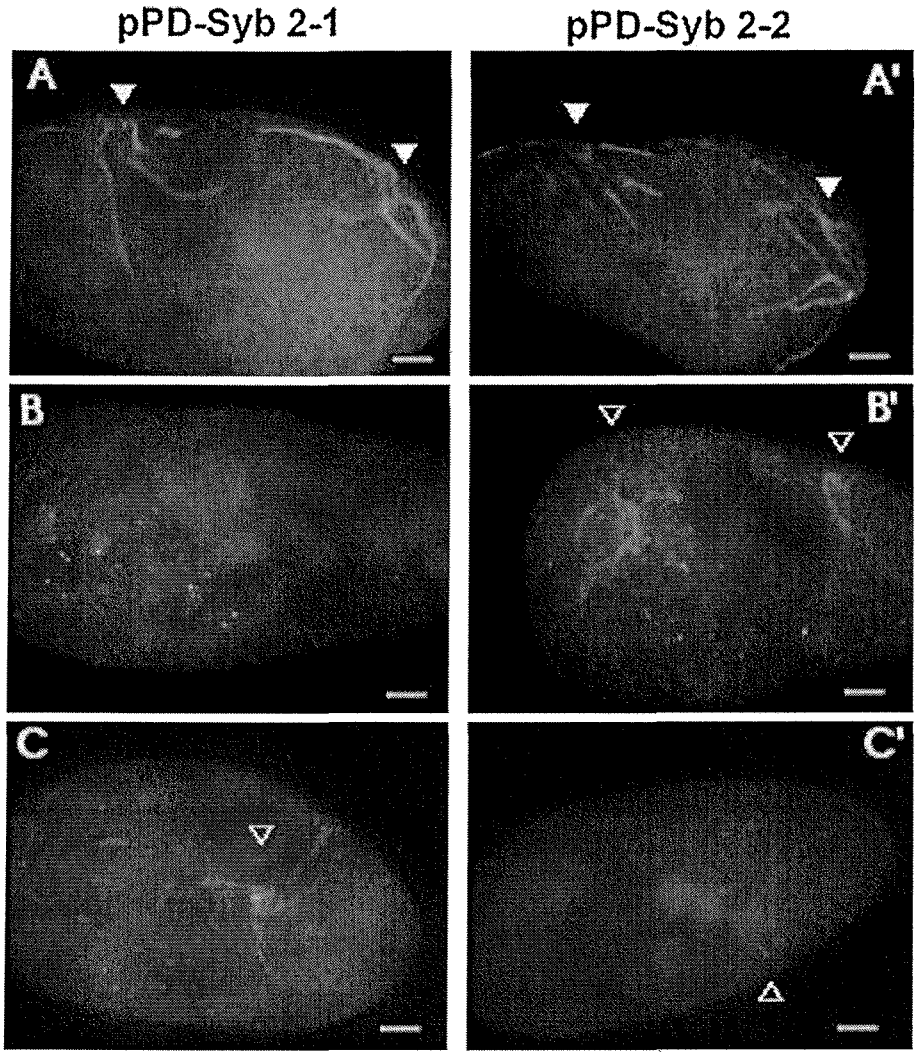

Fig. 5. Selective silencing of the two ohnologs, Syb2-1 (A–C) and Syb2-2 (A′–C′). In both series, the a2 SU of the H^+-ATPase persists (A and A′), in contrast to the Syb2 isoforms (B and B′) and the IP_3R (C and C′). Bars = 10 μm.

3.2. *Localization studies combined with silencing effects*

In Fig. 1 Syb2 labeling as a GFP-fusion protein shows a spotty appearance that extends from the CV over the radial arms and the smooth spongiome. While this focal enrichment may reflect vesicular transport or any other local activity discussed in Sections 4.3–4.5, AB labeling shows some variability, from spotty to smooth, with other SNAREs. CVC-resident SNAREs not previously localized encompass Syb6, Syb9 and Syx14. Using monospecific ABs we now have localized them to the CVC by the immuno-gold EM method (Fig. 2). They are all localized predominantly to the smooth spongiome, notably to its peripheral zones. No labeling of the decorated spongiome is seen. Controls without primary AB incubation resulted in no such labeling and labeling was normal in mock-silenced cells (data not shown).

To expand the analysis of SNAREs at the EM level to the broadest spectrum possible we performed silencing of the SNARE-specific chaperone, NSF (Fig. 3). Ultrastructural analysis revealed considerable structural reduction. In fluorescence analyses we saw that NSF silencing reduces staining of the CVC with ABs against non-SNARE CVC proteins, such as the SU a2 of the H^+-ATPase and the inositol 1,4,5-trisphosphate receptor (IP_3R) – both established components of the CVC (see Section 1). As a rule we saw highest sensitivity to NSF silencing with Syb2 ABs and lowest with Syx2 AB staining, while staining for other antigens was more variable after NSF silencing (data not shown). In summary, these pilot experiments suggest that SNAREs are involved in the delivery and/or positioning of widely different components of the CVC. Any effects of silencing, also of specific SNAREs (below), may therefore involve also non-SNARE components.

Which subdomains of the CVC are affected by NSF silencing? Fig. 3A depicts the normal appearance of a radial arm with its surrounding smooth spongiome and some elements of the decorated spongiome. The preponderance of the smooth spongiome is evident. After NSF silencing the amount of smooth spongiome profiles decreased, although it never obliterated totally (Fig. 3B and C), as does to some extent the decorated spongiome. Similar ultrastructural observations were made after silencing of organelle-resident SNAREs such as Syx2 (Fig. 6).

We then addressed the relevance of individual SNAREs by AB staining at the LM level. We investigated the effect of silencing of individual genes on the localization of the respective gene product and some of the other CVC-resident proteins (Figs. 4 and 5). To cope with the problem that gene silencing can result in barely

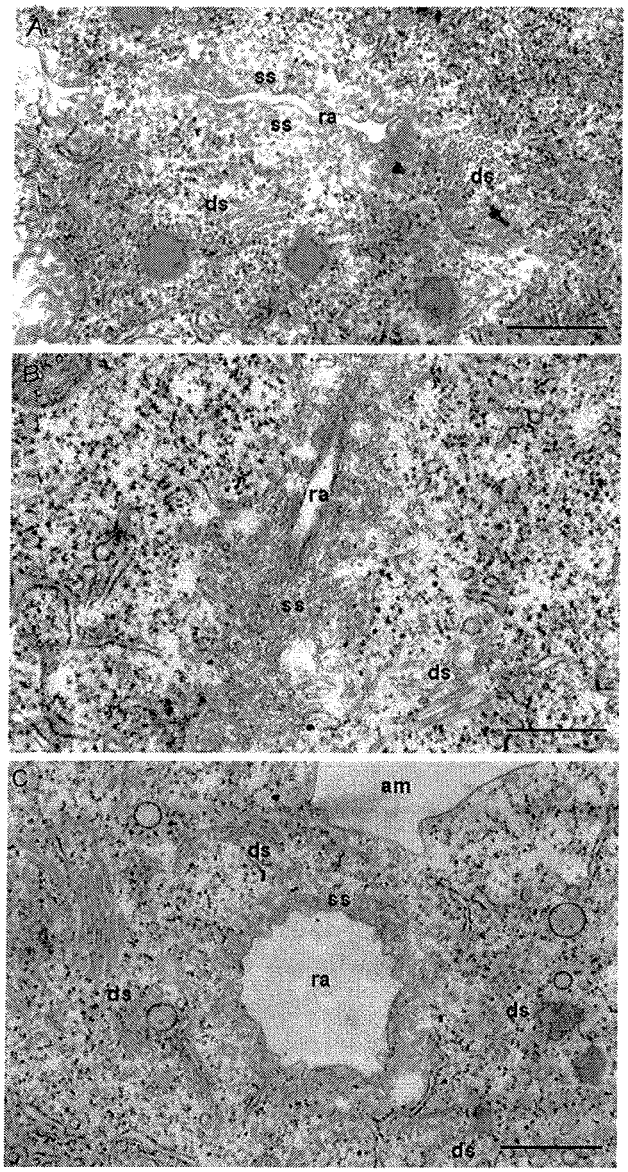

Fig. 6. Examples of the ultrastructural appearance of Syx2 silenced cells (A–C). Note variable obliteration of the smooth (ss) and decorated spongiome (ds) around the radial arms (ra); in (C) a radial arm is dilated, as is the ampulla (a) in (C). Bars = 0.5 μm.

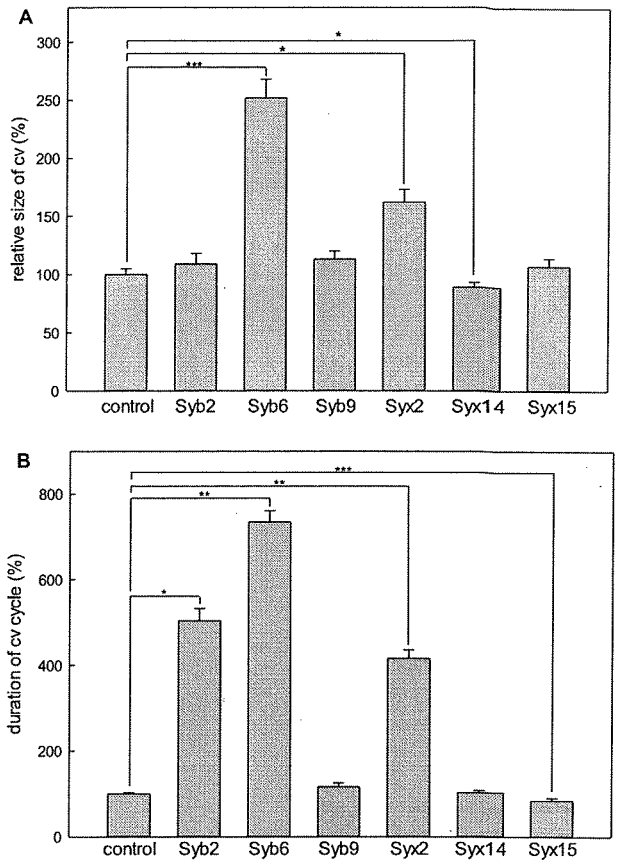

Fig. 7. CV area size relative to cell size (A) and duration of pumping cycle 65 h after silencing (data normalized to control after mock-silencing with empty PDX vector [100%]) shown in (B). The number of cells analyzed under the restrictions described in Section 2.5, i.e. strict median section of the CV and the respective cell, has been between 12 and 18 for each type of SNARE; data are representative for several independent silencing experiments. For viability a much larger number of cells has been evaluated (see Section 2.5). ± values indicate s.e.m. */**/*** indicate $p \leq 0.05/0.005/0.0005$ in Student's *t*-test, respectively. All cells remained fully viable under all conditions.

visible CVCs after AB staining or with the distortion of the organelle we eventually included staining with ABs against CVC-resident tubulin (Fig. 4). Staining with anti-tubulin ABs also served as a rather invariable standard to compare with staining achieved by ABs against CVC membrane proteins. Prerequisite is our experience that in most silencing experiments staining with anti-tubulin ABs remains associated with the CVC in a rather robust manner.

In non-silenced controls (empty pPD vector only) tubulin coincides with Syb2 staining (Fig. 4A and A′) and Syx2 (Fig. 4C and C′). Syb2 silencing greatly reduces staining with anti-Syb2 ABs (Fig. 4B and B′). In this series, silencing of Syx2 does reduce – to some extent and with some variability – staining with anti-Syx2 ABs (Fig. 4D and D′), but the outlines of the organelle still can be vaguely seen (compare encircled area in D′ with D). Syx2 silencing has no effect on staining with ABs against Syb2 (Fig. 4E and E′). No abolition by Syx2 silencing could be detected for staining with ABs against SU a2 of the H^+-ATPase (Fig. 4F and F′) and ABs against the IP_3R (Fig. 4G and G′). In summary, in this series, silencing of Syb2 results in the reduction of the staining for Syb2, whereas Syx2 silencing has less evident effect on Syx2 staining. This constellation has been frequently observed. Syx2 silencing also has little effect on the two non-SNARE proteins. Considering the similarity of the two Syx2 ohnologs (above) this may imply the relevance of t-/Q-SNAREs other than Syx2 for the delivery of H^+-ATPase SU a2 and IP_3R by vesicle trafficking. As mentioned above, Syb2-1 and Syb2-2 ohnologs diverge beyond the 85% limit assumed for co-silencing, so they have also been silenced separately.

Silencing of Syb2 was further specified for the two ohnologs, Syb2-1 and Syb-2, respectively (Fig. 5). Silencing of either Syb2 isoform greatly reduced staining for this antigen (ABs recognizing both ohnologs), although Syb2-2 was more resistant to silencing. Otherwise, regardless which ohnolog, Syb2-1 (Fig. 5A–C) or Syb2-2 (Fig. 5A′–C′), has been silenced the result was quite similar. Syb2-1 or Syb2-2 silencing had little effect on staining and arrangement for the a2 SU of the H^+-ATPase (Fig. 5A and A′). By contrast, staining for the IP_3R was greatly reduced (Fig. 5C and C′), particularly after Syb2-2 silencing (Fig. 5C′).

We have seen in numerous experiments that staining for the t-SNAREs Syx2 was less affected by silencing than that for the v-SNARE Syb2, although Syx2 silencing entails severe functional effects (Figs. 8 and 9). If the organelle-resident receptor SNARE Syx2

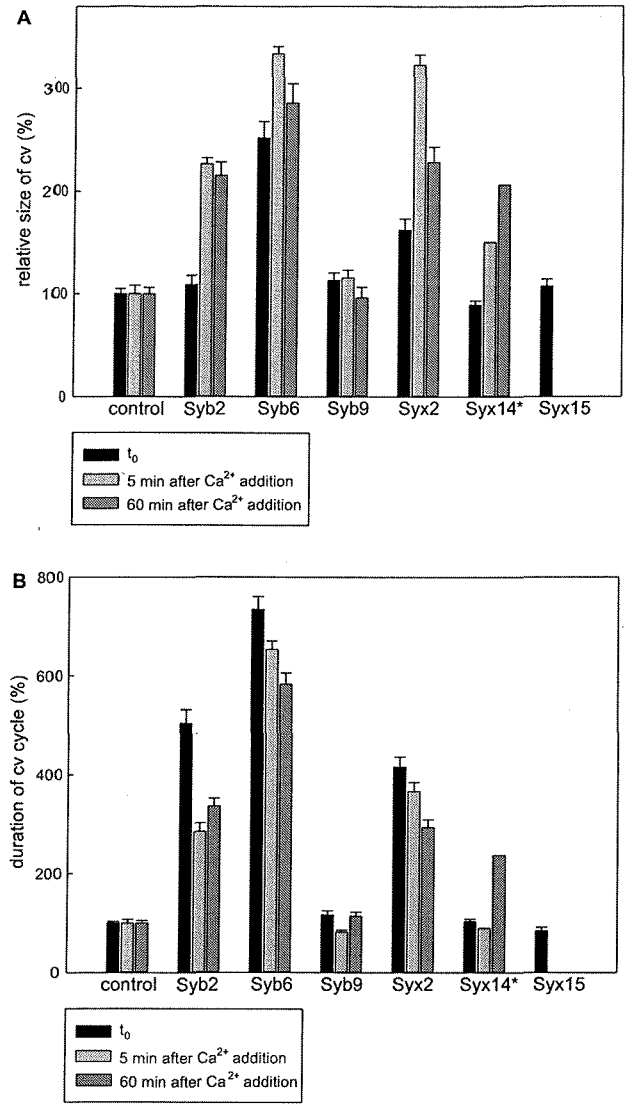

Fig. 8. CV size relative to cell size (A), duration of pumping cycle 65 h after silencing (data normalized to control, i.e. empty PDX vector mock-silencing) shown in (B). Recording was after silencing different SNARE genes, followed by Ca^{2+} stress (addition of 5 mM Ca^{2+} for up to 1 h). Viability was 100% for controls (analyzed without $[Ca^{2+}]_o$ increase) and Syb2 silenced cells (up to 60 min Ca^{2+} stress), Syb6 and Syb9 (5 min), Syx2 (up to 60 min Ca^{2+} stress) and Syx14 (5 min); it was 60% for Syb6 (60 min), 65% for Syv9 (60 min) and 50% for Syx14 silenced cells (30 min Ca^{2+} stress). Since some Syx14 silenced cells died within 30 min (asterisk) no statistic data are given, and no Ca^{2+} stress data can be given for cells silenced in Syx15 as they died rapidly within 2–3 min exposure to Ca^{2+} stress. For each of the silenced SNARE and the the respective times of Ca^{2+} stress, 12–18 cells (representative for several independent experiments) have been analyzed under the restrictions described in Section 2.5. Note that for viability a much larger number of cells has been evaluated (see Section 2.5). % values are referred to controls, i.e. mock-transfected cells with Ca^{2+} exposure for the same time (including time showing maximal effect). ± bars indicate s.e.m. For Student's t-test see text in Section 3.4.

is less affected than the vesicular delivery SNARE, Syb2, why are functional effects severe? Does Syx2 silencing entail any effects at the ultrastructure level not recognized in the LM? In the EM the smooth spongiome was reduced to a varying, but not severe extent, as documented in Fig. 6A–C. In Fig. 6C a swollen radial arm is surrounded by more or less profiles of the smooth spongiome. This is compatible with a transformation of these interconvertible membranes, from planar to tubular and reverse and it does not contradict that its t-SNARE Syx2 is still present. Also note in Fig. 6

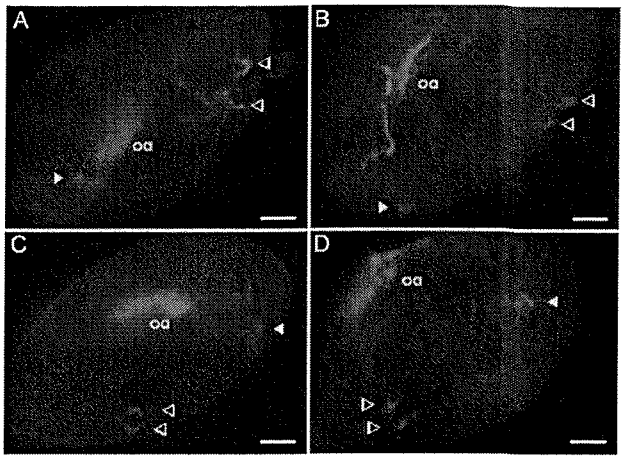

Fig. 9. Four examples (A–D) of consequences of Syx6 silencing on CVC positioning visualized by anti-tubulin AB staining (which also stains the oral apparatus, oa). In (A) a larger and a smaller CVC (or rather their microtubular scaffold) are seen side by side (arrowheads, top right), in addition to a star-shaped CVC outline (lower left). (B and C) shows three CVCs, of which two small ones are relocated side by side (arrowheads); single ones occur in all these examples, e.g. at the bottom left in (B) and at the top right in (C) and (D). In addition to the fragmentary appearance of the small CVC pairs, also note the atypical localization lateral to each other (C and D). Bars = 10 μm.

the presence of elements of the decorated spongiome, though in reduced quantity – as well as of the IP_3R and of the H^+–ATPase in Fig. 4 (prerequisite to Ca^{2+} regulation). We try to reconcile these discrepancies between absent to moderate structural details and the pronounced functional effects of Syx2 silencing (Figs. 8 and 9) in Sections 4.3 and 4.4.

3.3. *Effects of gene silencing on the function of the CV*

We tested the effect of silencing of those Syb- and Syx-type genes which, according to immuno-localization, occur in the CVC and, thus, may probably be relevant for its function. In precisely cross-sectioned cells with precisely cross-cut CVs from video series (see Section 2) we measured cell size, CV size (area size, absolute and in relation to cell size, at the time of maximal expansion before systole), and duration of the contraction cycle, all after 65 h silencing of the respective genes. For controls the empty pPD vector was applied for the same time. We started with experiments at standard $[Ca^{2+}]_o = 1$ mM.

First, the effect of NSF silencing on the contraction cycle of the CV has been analyzed. It results in an increased duration by a change from 100 ± 13% (s.e.m., standard error of the mean), as defined for controls, to 220 ± 42% (unpubl. results). Second, we have investigated the effect of silencing specific SNAREs on the size of the CV and on the contraction cycle (Fig. 7). The effect of silencing in standard medium on CV size is not very much pronounced with Syb2 and Syb9, Syx14 and Syx15, with no significant difference for Syb2, Syb9 and Syb15. There is some significance only for Syb6, Syx2 and Syx14 when compared to controls. The duration of the contraction cycle is little affected in cells silenced for Syb9, Syx14 and Syx15, whereas significant differences occur with Syb2, Syb6 and Syx2. The silencing effect of Syb15 was small but significant. Strikingly, after Syb2 silencing the CV maintains its size, but it works much more slowly than in controls. The most severe, statistically significant responses in CV size and contraction activity occur after silencing Syb6. In sum, this makes particularly Syb2, Syb6 and Syx2 appear important for CVC performance. Both parameters, CV size and pumping activity are least affected after silencing Syx14 and

Syx15 although their silencing yields the strongest effect in the Ca^{2+} stress test (below).

3.4. Ca^{2+} stress experiments

Next, after 65 h silencing for different SNAREs, cells were subjected to Ca^{2+} stress by increasing $CaCl_2$ in the medium to 5 mM (Fig. 8). The evaluation method was as described above and in Section 2.5. For additional controls we also probed osmolytes other than Ca^{2+}. Within a period up to 1 h the same parameters were measured as for the time before $[Ca^{2+}]_o$ increase. Data determined in Fig. 7 after 65 + 1 h gene silencing without additional Ca^{2+} ($[Ca^{2+}]_o = 1$ mM) served as "control i". In additional controls non-transformed cells were exposed to $[Ca^{2+}]_o$ increased to 5 mM (control ii). In further controls cells contained in the control medium with 1 mM $CaCl_2$ were supplemented with each 5 mM of $MgCl_2$ (control iii), lysine (control iv) or 2-deoxyglucose (control v), each 5 mM. Per assay at least 10 cells (in strict median section) have been evaluated. In this sequence, mean values for the contraction cycle were 9.3 ± 0.4 s (s.e.m.) in control (i), 11.9 ± 2.1 s (ii), 8.9 ± 0.5 s (iii), 7.5 ± 0.4 s (iv), and 9.4 ± 0.4 s (control v), respectively. When "control i" is normalized to 100 ± 4%, values for the other controls are 128 ± 23% (ii), 96 ± 5% (iii), 81 ± 4% (iv), and 101 ± 4% (control v). There was no statistically significant difference ($p > 0.05$ in all cases). In the same sequence, the relative area size of the CV at its maximal expansion changed as follows (referred to control i = 100%): 100 ± 8% (s.e.m.; control [ii]), 101 ± 6% (iii), 110 ± 7% (iv), and 135 ± 7% (control v), again without any significant statistical difference. In sum, changes induced by Mg^{2+}, lysine or 2-deoxyglucose are only marginal and cannot explain the effects achieved by increasing $[Ca^{2+}]_o$ to 5 mM, also for 1 h, in the following experiments.

The Ca^{2+} stress test reveals different sensitivity depending on which SNARE had been silenced (Fig. 8). Cells essentially react to all silencing conditions, but to a different extent in a different time sequence; any changes involved CV swelling. Under Ca^{2+} stress, in Syb2 silenced cells the size of the CV increases within 5 min to 226 ± 6% (s.e.m.) relative to the control (=100%; Syb 2 silenced without increased $[Ca^{2+}]_o$); this changes only slightly to 215 ± 13% within 1 h. In Syb6 silenced cells an increase to 334 ± 17% is seen already after 5 min; it goes slightly down to 286 ± 19% within 1 h. All these changes were statistically significant ($p \ll 0.05$). After Syb9 silencing the slight increase to 115 ± 8% within 5 min is followed by a reduction to 96 ± 10% within 1 h Ca^{2+} stress. This was the only reduction observed, though it was not statistically significant, as was the increase after 5 min. Syx2 silencing increases CV size within 5 min to 323 ± 10%; this goes down to 228 ± 15% within 1 h; for these changes a $p \ll 0.05$ was determined in relation to controls. Syx14 silencing caused an increase to 150% within 5 min and further increase to 206% within 30 min. No 1-h-value was determined as these cells rapidly lost their viability in the Ca^{2+} stress test medium. This was even more pronounced with cells silenced in Syx15 which entails greatly reduced viability already within minutes in increased $[Ca^{2+}]_o$ medium. We therefore abstained from any further evaluation. By contrast, cells silenced in the other SNAREs well survived the Ca^{2+} stress test and, in pilot experiments, values changed to those determined before increasing $[Ca^{2+}]_o$.

Silencing of the different CVC-resident SNAREs, in combination with Ca^{2+} stress, also affected the CV pumping frequency, though less than silencing alone. In comparison to controls (100%), Syb2 silencing results in a change to 285 ± 17% (5 min), followed by further increase to 336 ± 16% (1 h). This was by far exceeded by Syb6 silencing, resulting in 654 ± 17% after 5 min and 583 ± 23% after 1 h, thus indicating some slight compensation with time. Syb9 silencing had little effect, i.e. a reduction to 82 ± 4% (5 min), followed by a slight increase to 114 ± 8% (1 h), though the difference between 5 and 60 min was not statistically significant. With Syx2 the immediate effect was much higher (366 ± 19%, 5 min) from where it then slightly declined to 293 ± 16% (1 h). Syb 14 silenced cells reacted more slowly to the Ca^{2+} stress; after 5 min the contraction cycle time was slightly reduced to 90%, but then it increased to 237% within 30 min. There we stopped evaluation because of reduced viability. The rapid deterioration of Syx15 silenced cells again precluded any evaluation.

3.5. Observations on de novo CVC biogenesis

A frequent observation was that Syb6 silencing causes misplacing of de novo formed CVCs as seen by staining of the organelle-resident microtubules (Fig. 9). In close association with existing CVCs new ones are seen, yet located either at the posterior or at a lateral side of the maternal one. In some cells two newly formed CVCs also occurred in close association with each other. Selected examples are presented in Fig. 9. Less frequently we observed two or up to three small CVCs after Syx2 silencing.

4. Discussion

4.1. Essential aspects of the present work

The goal of our work was to analyze the importance of SNAREs for structure and function of the CVC of *Paramecium*, focusing on the relevance for Ca^{2+} tolerance. From the large repertoire of SNAREs found in the CVC of *Paramecium* [42,43] we find essentially each three v-/R- and t-/Q-SNAREs. This includes Syb2, Syb6 [38] and Syb9 [40] as well as Syx2, Syx14, and Syx15 [41]. Their restriction to this organelle – except the additional Qa/b-SNARE, SNAP25-like protein (LP) [39] – suggests important functions for which we now see several possibilities. Remarkably, data on SNAREs in the CVC of other organisms are very scarce. Syx7 sequences are found in the *Dictyostelium* genome [7], as are some hypothetical proteins called SNARE2.1, SNARE2.2 and VAMP in *T. cruzi* [12].

4.2. Which possible functions could SNAREs exert in the CVC?

4.2.1. Where SNAREs occur

Using immuno-fluorescence under appropriate conditions, NSF can be seen highly concentrated at sites of established membrane fusion activity, i.e. the porus and the onset of radial arms on the CV [37]. However, less intense staining also spreads over the organelle. The SNAREs described here are generally distributed broadly over different parts of the CVC, again except the decorated spongiome. Only some, i.e. Syb2, Syb9, Syx2 and Syx15, also occur at the porus (Fig. 10). From this localization and the functional needs now to be discussed we may envisage SNARE involvement principally in widely different activities.

4.2.2. Which SNARE functions to envisage

There are many possibilities. (i) The relevance of SNAREs for CV/cell membrane fusion (exocytosis) and (ii) for radial arms/CV fusion is obvious since membrane capacitance changes have been registered during these processes, including CV/ampullae dis-/reconnection [51]. (iii) In a steadily ongoing renewal, a "cryptic" biogenetic process, a multitude of membrane proteins has to be delivered by vesicular transport. (iv) "Overt" biogenesis, i.e. de novo formation before cell division, will also depend on SNAREs, as does positioning of CVC. Whereas these aspects are well founded, the following aspects, though speculative, may help understanding the widely different effects of SNARE silencing per se and in a combination of silencing and Ca^{2+} stress. (v) The labyrinth of spongiome tubules may involve stochastic fusions and disconnections,

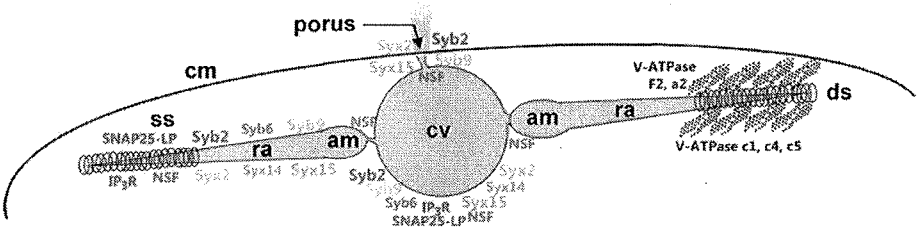

Fig. 10. Distribution of molecular components in the CVC of *Paramecium*. *Abbreviations*: am = ampullae, cv = contractile vacuole, ds = decorated spongiome, ra = radial arms, ss = smooth spongiome. Data summarized from the present work as well as from previous work: Syntaxins [41], Synaptobrevins [38,40] and SNAP25-like protein designated SNAP [39], in addition to NSF [37] and the IP_3R [28] are scattered over the entire CVC except the decorated spongiome. SUs of the H^+-ATPase (V-ATPase [17,18]) are restricted to the decorated spongiome (right). Only selected SNAREs are visibly concentrated at the porus (top).

though this has been ascertained so far only for smooth/decorated spongiome elements under hyperosmotic conditions [52]. SNAREs may, thus, mediate transient de-/re-coupling of parts of the spongiome depending on physiological requirements. Note that also fission depends on SNAREs [53]. (vi) The tight packing of spongiome tubules particularly in the smooth spongiome may require trans-SNARE complexes as an organizing factor. Note that non-fusogenic SNAREs, as known from higher eukaryotes [54], may be involved. (vii) The periodic rearrangement of CV and radial arms membranes, from planar to tubular/vesicular and reverse during systole/diastole transition may involve SNAREs. In fact, transformation of a labyrinth into a smooth membrane is an challenging unsolved problem. (viii) Some SNAREs associate with specific membrane proteins and thus determine their targeting. For instance, in mammalian systems specific cation channels [55], including some Ca^{2+}-channels [56] and H^+-V0 subunits [57] interact each with specific SNAREs for delivery to the respective target membrane [58]. Since a ΔH^+ drives Ca^{2+} sequestration, lack of some CVC-resident SNAREs may increase sensitivity in the Ca^{2+} stress experiments. In summary, one can expect many SNARE functions, particularly in a complex organelle, such as the CVC. Among the hypotheses mentioned, (i) to (iv) are well supported by our own and (viii) by published data, whereas (v)–(vii) are postulates to be tested in future work.

4.2.3. SNAREs located at specific sites and functional consequences

SNAREs located at the porus (Fig. 10) are candidates for CV exocytosis regulation. Some other SNAREs may mediate the periodic d-/re-connection of ampullae with the CV [51]. Although difficult to "catch" by labeling with ABs against specific SNAREs, both these sites can be intensely labeled with ABs against NSF provided care is taken to retain NSF molecules [37] which normally associate only transiently with their site of activity [36]. No such clear function can currently be assigned to any of the SNAREs in other parts of the organelle.

Since Syb6, in contrast to Syb2 and Syx2, is not visible at the porus (Fig. 10), the most serious swelling observed after Syb6 silencing, before and during Ca^{2+} stress, cannot simply result from impaired CV fusion activity, but must result from an effect deeper inside the CVC. Also pulsation activity is considerably reduced. This would match hypothesis (viii). Cells silenced in Syb2 or Syx2 were sensitive to silencing of the respective SNAREs already before the Ca^{2+} stress test. These two have the broadest distribution and, thus, may be active in any part of the CVC. For the discrepancy between (ultra)structural and functional effects of Syx2 silencing, see below.

Syb9 silenced cells are little sensitive under conditions of normal and increased $[Ca^{2+}]_o$ though it also occurs at the porus. This suggests either more subtle microdomain localization and function at the porus and/or some mutual functional complementation by other SNAREs in the porus region. The reduced viability after Syx14 silencing under Ca^{2+} stress is surprising because silencing before adding additional Ca^{2+} had only little effect on CV size ($89 \pm 4\%$) and activity ($103 \pm 5\%$) and only a 206% effect was measured after 30 min $[Ca^{2+}]_o$ increase. This SNARE may, therefore, also be involved specifically in Ca^{2+} dynamics. The weak response in CV size ($107 \pm 7\%$) and pulsations ($84 \pm 7\%$) after Syx15 silencing is in contrast to the deleterious effect of Ca^{2+} stress in these cells within minutes. Its occurrence at the CV porus (in addition to regions deeper inside the CVC; Fig. 10) can explain obstruction and cell death by acute Ca^{2+} intoxication. In summary, one can argue about manifold functions of the different CVC-resident SNAREs. Some other aspects can be more clearly defined, as follows.

4.3. Potential role of SNAREs in protein delivery and CVC biogenesis

4.3.1. Evidence based on previous work

"Cryptic" biogenesis serves the steadily ongoing replacement of molecular constituents although one cannot directly observe vesicle trafficking to this organelle. The frequently seen punctate labeling with ABs against SNAREs in the CVC (Fig. 1), occasionally also outside the organelle, may reflect vesicle delivery. There is only indirect and rather anecdotal evidence of CVC biogenesis by vesicle trafficking in other systems, e.g. in *Dictyostelium* [59]. More conclusive is the occurrence of Rab-type GTPases that are known to be important for CVC function [60]. They occur in the CVC of *Dictyostelium* [11], *Tetrahymena* [45] and *Paramecium* [61]. Components of the exocyst, a multimeric complex mediating vesicle docking, are reported from *Chlamydomonas* [62] and *Dictyostelium* [63].

After NSF silencing we observe in the EM a decreasing structural complexity of the spongiome (Fig. 3). By immuno-fluorescence we see, also after NSF silencing, a decreased labeling of the CVC with ABs against Syb2 and frequently of IP_3Rs and H^+-ATPase SU a2 (data not shown). The reduction of these proteins is compatible with the assumption of their delivery to the CVC by ongoing vesicle trafficking.

4.3.2. SNARE silencing and functional effects

According to our silencing experiments Syb2 plays a crucial role. Syb2 [38], Syx2 [41], Syb6, Syb9 and Syx14 (this study) were found by immuno-gold localization mainly at the periphery of the smooth spongiome (Fig. 2). There they could mediate the docking of vesicles engaged in "cryptic" biogenesis and their silencing could thus affect the delivery of other essential CVC proteins. Particularly Syb6 silencing affects normal CVC activity (Fig. 7) whereas Syx14 and Syx15 silencing causes extreme sensitivity to Ca^{2+} stress (Fig. 8). These effects may be rather indirect. For instance, IP_3Rs as well as SUs of the V0 part of the H^+-pump are engaged in Ca^{2+} homeostasis in *Paramecium* [64] and both are delivered by SNARE-dependent

trafficking. In mammalian cells IP_3Rs are detected in the ER and the Golgi apparatus in mammals [65]; from there, in the *Paramecium* cell, they may be delivered to the CVC. In mammals, the H^+-ATPase delivery occurs in association with a Syx-type SNARE [57]. One may envisage SNAREs also for delivery of some putative components (cation antiporters and aquaporins) of functional importance. All this would make CVC functions, including handling of Ca^{2+}, highly dependent on SNARE functions. The delivery of such vesicles may occur anywhere below the decorated spongiome where the densely packet pegs of the H^+-ATPase [15–18,24] would hinder vesicle docking. Concomitantly any SNAREs localized at the EM level, show up only below the decorated spongiome.

Also Syb2 is important for the localization of IP_3R, though with some variability. Individual silencing of the ohnologs, Syb2-1 and Syb2-2, has a severe effect on IP_3R, but little effect on positioning the H^+-ATPase SU a2 (Fig. 5). This implies they cannot substitute for each other (Fig. 5). Since for differential silencing a similarity at the nucleotide level of about 85% is a generally accepted upper limit [46] and since the two Syb2 ohnologs resemble each other by only 81% [38] we were not sure to expect this effect. One possibility would be that the two ohnologs affect two different steps of vesicle delivery to the CVC.

How to reconcile the considerable retention of smooth (and decorated) spongiome, and molecules important for Ca^{2+} regulation residing in it, after Syx2 silencing (Fig. 6) with the considerable effect of Syx2 silencing on CVC performance before (Fig. 7) and during the Ca^{2+} stress test (Fig. 8)? Failure in IP_3R delivery cannot be the cause as it is still present in the CVC (Fig. 4G and G′), as is the H^+-pump SU a2 (Fig. 4F and F′). This is supported by the fact that inhibition of IP_3R synthesis and delivery after IP_3R silencing causes severe reduction of the smooth spongiome in EM analyses (data not shown), but this is not so after Syx2 silencing. We propose as a hypothesis that Syx2 may be important for the delivery of other important components, among them possibly aquaporins and or cation antiporters. Both are hypothetic for the *Paramecium* CVC, but under discussion in other systems (see Section 1).

4.4. Possible structural effects of SNAREs on CVC dynamics

4.4.1. SNAREs of different importance

The effect of silencing in standard medium, $[Ca^{2+}]_o = 1$ mM, with regard to CV size and pulsation frequency, is highest with Syb6, followed by Syb2 and Syx2 (Fig. 7). Similarly, in the Ca^{2+} stress test, sensitivity is highest for cells silenced in Syb6, followed by Syx2 and Syb2 (disregarding Syx14 and Syx15 silenced cells which survive only shortly). Therefore, these SNAREs may be most important for ongoing CVC activity – but how?

4.4.2. Reversible membrane tubulation

During systole, the projection area of a CV – if it were still visible in the LM – should double when it collapses to a disc (which for optical reasons cannot be seen). However, the EM reveals that the CV undergoes massive transformation into 40 nm thick tubules [30,66,67], i.e. the smooth spongiome. Ampullae as well as the onset of the canals are also prone to transient tubulation and vesiculation in the collapse phase [51] – phenomena reported also from other protists [59]. Tubulation appears essential for accommodating the excess of membrane for re-use in diastole, when membranes are smoothened out and, thus, make the CV again visible in the LM. Collapse by tubulation after systole and rounding up during diastole also occurs in *Dictyostelium* [7]. Thus, the total membrane area can be maintained when CV, ampullae and radial arms collapse, until chemiosmotic pressure restructures these membranes during diastole. This matches the fact that lipid bilayers tolerate only little expansion or compression [68,69] – a fact applicable also to hypotonic organelle swelling [70]. Clearly re-integration of such tubules and vesicles is required in order to re-establish a round CV during diastole.

All of the bizarre membrane deformations occurring during systole must somehow be regulated. It may be one function of SNAREs to locally impose a tubular form by formation of trans-complexes; canceling of such restriction would then allow CV enlargement during diastole. Consequently swelling of the CV under experimental conditions (Figs. 7 and 8) would consume more or less of the smooth spongiome, as we can actually observe in the EM. Under physiological conditions, within the spongiome, branched tubules might be dis- and re-connected via SNARE activity depending on osmotic conditions, just like Rab-mediated interactions between yeast vacuoles [71]. During tubulation the CV, ampullae and radial arms remain attached to the microtubule corset [30] whose spiral arrangement may facilitate flattening and refilling.

Since no biomembrane undergoes spontaneous tubulation this requires specific mechanisms. Specific membrane bending proteins are required, such as F-BAR in mammalian cells [72]. In fact, in *Dictyostelium* F-BAR proteins are bound to the CV during its discharge, thus causing tubulation [73]. In addition MEGAP-type proteins regulate curvature and tubulation in the CVC [73]. Equivalents still await detection in *Paramecium*. These expectations are supported by additional observations with mammalian cells. Tubulation occurring during endocytosis and membrane recycling requires specific Rab-type GTPases, such as Rab11. Rab11 occurs in the CVC of *T. cruzi* [12] and of *Dictyostelium* [11]. In *Dictyostelium* its expression level determines the size of the CV [74]. In *Tetrahymena* Rab proteins have been localized as GFP-fusion proteins; here Rab11 was found only in endosomal compartments, whereas some other Rabs were seen in the CVC [45]. However, in *Paramecium* 14 Rab11 forms occur, with 4 singletons and 5 pairs [61], thus indicating considerably larger diversification. Rab11 is known to cooperate with SNAREs in targeted vesicle trafficking [75]. All this now calls for detailed localization and functional analysis. A connection of the CVC to endocytosis has been propagated for *T. cruzi* [12] and *Dictyostelium* [6], but not yet for ciliates. Remarkably, in mammals, tubulation, e.g. of endosomes, occurs along microtubules, as it also occurs in the CVC in *Paramecium*. What could the relevance of these arguments be for CVC performance, e.g. for Ca^{2+} stress tolerance?

Is it feasible to consider the smooth spongiome a reservoir for CV swelling? Consider the extreme swelling of the calculated volume in cells silenced for Syb6 to 735% of its original size and to an additional 334% during Ca^{2+} stress (Fig. 8). Also consider the very small extensibility of biomembranes [67,68] and the unlikelihood of any substantial membrane delivery within the short times of a Ca^{2+} stress test. As determined in *Paramecium multimicronucleatum* by Tominaga et al. [30], the CV surface area is $2 \times 10^3\ \mu m^2$, whereas the total CVC membrane area is estimated as $18 \times 10^3\ \mu m^2$. If one assumes an area of $\sim 2 \times 10^3\ \mu m^2$ also for radial arms this would leave $\sim 14\ \mu m^2$ for the remaining CVC membrane area, thereof 90% for the smooth (according to a rough estimation of profiles seen in the EM). This would just suffice for an increase of the CV volume to the size actually observed. For further enlargement during Ca^{2+} stress transformation of decorated spongiome appears required, as reflected by its decrease, e.g. in EM micrographs after NSF silencing. Remarkably some change in structure and function in the decorated spongiome is possible under experimental conditions [76]. From all this we conclude that the smooth spongiome (less the decorated spongiome) can indeed serve as a membrane reservoir during extreme osmotic conditions. For the transformation of a 3D tubular network one inevitably has to assume breakup of 3D connections to form non-branching tubules which can be smoothened out during diastole. This interplay is an intriguing, unresolved problem of membrane biology, with SNAREs as

potential key-players for tolerance to osmotic conditions and increased $[Ca^{2+}]$ in the environment.

4.5. Possible effects of SNAREs and CRCs on Ca^{2+} dynamics

4.5.1. CVCs are important for $[Ca^{2+}]_i$ homeostasis

In *Dictyostelium* it has been calculated that 70% of the $^{45}Ca^{2+}$ permeation is counterbalanced by the CVC within 15 min [77]. In *Paramecium* the compensation time in the sequence of Ca^{2+}-stimulated exocytosis is estimated as ~6 min [28]. Clearly these rough estimations assign to the CVC an important role for $[Ca^{2+}]_i$ regulation. This may be even more demanding, considering that Stock et al. [21] show a $[Ca^{2+}]$ of 15–30 mM in the CV of *P. multimicronucleatum* when outside osmolarity is increased to 24 and 125 mOsmol/L, respectively. That Ca^{2+} sequestration into the CV is linked to H^+-ATPase activity becomes evident from its down-regulation by an anti-sense RNA strategy which greatly reduces Ca^{2+}-transport by the CVC in *Dictyostelium* [78]. Similarly inhibition of the H^+-ATPase in *Paramecium* prolongates $[Ca^{2+}]_i$ downregulation after massive synchronous exocytosis stimulation by a factor of ~10 [64].

4.5.2. Feedback from CVC function to other functions

Beyond its importance for secreting Ca^{2+}, the activity of the CVC can conversely be assumed to be governed by the local availability of Ca^{2+}. The CVC of *Paramecium* possesses several types of CRCs. CRC-II represents true IP_3Rs scattered over the entire CVC except the decorated spongiome [28]. Its constitutive activity serves fine-tuning of $[Ca^{2+}]_i$ by partial reflux. When this CVC component is downregulated, basic Ca^{2+}-dependent cell functions are impaired, as exemplified by the biogenesis of dense core-secretory organelles, the trichocysts [79]. Less well analyzed are three additional CRCs [29]. Type CRC-V-4 is localized to the CV and the radial arms (no EM data being available). Interestingly CRC-VI-2 and CRC-VI-3 are localized at/around the porus region (the precise membrane/compartment being unknown). Since CRCs are generally positioned at strategic sites requiring Ca^{2+} signaling also in *Paramecium* [43] this strongly suggests a role in different CVC functions, with a feedback between Ca^{2+} sequestration/extrusion and reflux into the cytosol for fine-tuning. As mentioned, some SNAREs are located at the porus (Fig. 10) and, thus, available for fusion of the CV with the cell membrane in a kiss-and-run mode.

The following feedback may also be envisaged. In *Paramecium* an isoform of Stomatin has been localized to the CV, to radial arms and to the porus (A. Reuter, C.A.O. Stuermer, H. Plattner, submitted for publication). Over a range of eukaryotes Stomatin is indicative of mechano-sensitive Ca^{2+}-channels which it somehow regulates [80]. Among these, TRP- [81] and Piezo-type channels [82] are found in the *Paramecium* genome [64]. It is logical to assume sensor molecules for monitoring the filling state during chemiosmotic swelling and final discharge, as proposed already for *Dictyostelium* [11]. The tension of 5×10^{-3} N/m in the *Paramecium* CV [66] is close to that reported for such channels in other systems (http://www.ks.uiuc.edu/Research/MscLchannel/and [83]). It is not known as yet which Ca^{2+} channels and which SNAREs contribute at which site and in which phase to CVC activity. As mentioned, in some silencing experiments cells round up and become sensitive to increasing $[Ca^{2+}]_o$ (Fig. 8). Assuming a positive feedback between impaired handling of Ca^{2+} and severe effects on CVC activity agrees with the general assumption that $[Ca^{2+}]_o$, $[Ca^{2+}]_i$ and cell swelling are mutually interdependent [84].

4.6. Positioning of de novo formed CVCs

A rather unique, though consistent observation was the misplacement of newly formed CVCs occasionally after Syx2 (Fig. 4D and D') and more consistently after Syb6 silencing (Fig. 9), as evidenced by the misplacement of CVC-resident microtubules. Prerequisite for normal de novo formation may be extension of these SNAREs out to the tips of the radial arms. Indirect effects also appear feasible since cells are very sensitive for these two SNAREs. In the future this may give a handle to the analysis of epigenetically controlled positioning of this organelle [23].

4.7. Conclusion

The occurrence of SNAREs, of a Ca^{2+} sequestration mechanism and the availability of CRCs over vast areas of the CVC in *Paramecium* make this organelle a complex and highly efficient regulator of Ca^{2+} homeostasis. SNAREs and Ca^{2+}-mediated processes can govern a variety of specific CVC functions, from biogenesis, dynamic membrane restructuring to vesicle docking and fusion processes, including CV exocytosis. Which SNAREs execute which function at any specific site remains to be scrutinized.

Acknowledgements

We acknowledge the contribution by Drs. Eva-Maria Ladenburger, Thomas Wassmer and Christina Schilde and by advanced course students to this work at its early stage. This study has been supported by the Deutsche Forschungsgemeinschaft (grants to H.P.).

References

[1] R.D. Allen, Y. Naitoh, Osmoregulation and contractile vacuoles of protozoa, International Review of Cytology 215 (2002) 351–394.
[2] J.A. McKanna, Fine structure of the contractile vacuole pore in *Paramecium*, Journal of Protozoology 20 (1973) 631–638.
[3] R.D. Allen, The contractile vacuole and its membrane dynamics, Bioessays 22 (2000) 1035–1042.
[4] D.J. Patterson, M.A. Sleigh, Behavior of the contractile vacuole of *Tetrahymena pyriformis* W: a redescription with comments on the terminology, Journal of Protozoology 23 (1976) 410–417.
[5] R.D. Prusch, P.B. Dunham, Contraction of isolated contractile vacuoles from *Amoeba proteus*, Journal of Cell Biology 46 (1970) 431–434.
[6] J. Heuser, Q. Zhu, M. Clarke, Proton pumps populate the contractile vacuoles of *Dictyostelium* amoebae, Journal of Cell Biology 121 (1993) 1311–1327.
[7] G. Gerisch, J. Heuser, M. Clarke, Tubular-vesicular transformation in the contractile vacuole system of *Dictyostelium*, Cell Biology International 26 (2002) 845–852.
[8] K. Hausmann, D.J. Patterson, Contractile vacuole complexes in algae, in: W. Wiesner, D. Robinson, R.C. Starr (Eds.), Compartments in Algal Cells and Their Interaction, Springer-Verlag, Heidelberg, 1984, pp. 139–146.
[9] K. Buchmann, B. Becker, The system of contractile vacuoles in the green alga *Mesostigma viride* (Streptophyta), Protist 160 (2009) 427–443.
[10] P. Rohloff, R. Docampo, A contractile vacuole complex is involved in osmoregulation in *Trypanosoma cruzi*, Experimental Parasitology 118 (2008) 17–24.
[11] F. Du, K. Edwards, Z. Shen, B. Sun, A. De Lozanne, S. Briggs, R.A. Firtel, Regulation of contractile vacuole formation and activity in *Dictyostelium*, EMBO Journal 27 (2008) 2064–2076.
[12] P.N. Ulrich, V. Jimenez, M. Park, V.P. Martins, J. Atwood, K. Moles, D. Collins, P. Rohloff, R. Tarleton, S.N. Moreno, R. Orlando, R. Docampo, Identification of contractile vacuole proteins in *Trypanosoma cruzi*, PLoS ONE 6 (2011) e18013.
[13] E. Nishihara, E. Yokota, A. Tazaki, H. Orii, M. Katsuhara, K. Kataoka, H. Igarashi, Y. Moriyama, T. Shimmen, S. Sonobe, Presence of aquaporin and V-ATPase on the contractile vacuole of *Amoeba proteus*, Biologie Cellulaire 100 (2008) 179–188.
[14] A.K. Fok, M. Clarke, L. Ma, R.D. Allen, Vacuolar H^+-ATPase of *Dictyostelium discoideum*. A monoclonal antibody study, Journal of Cell Science 106 (1993) 1103–1113.
[15] A.K. Fok, M.S. Aihara, M. Ishida, K.V. Nolta, T.L. Steck, R.D. Allen, The pegs on the decorated tubules of the contractile vacuole complex of *Paramecium* are proton pumps, Journal of Cell Science 108 (1995) 3163–3170.
[16] A.K. Fok, K. Yamauchi, A. Ishihara, M.S. Aihara, M. Ishida, R.D. Allen, The vacuolar-ATPase of *Paramecium multimicronucleatum*: gene structure of the B subunit and the dynamics of the V-ATPase-rich osmoregulatory membranes, Journal of Eukaryotic Microbiology 49 (2002) 185–196.
[17] T. Wassmer, M. Froissard, H. Plattner, R. Kissmehl, J. Cohen, The vacuolar proton-ATPase plays a major role in several membrane-bounded organelles in *Paramecium*, Journal of Cell Science 118 (2005) 2813–2825.
[18] T. Wassmer, R. Kissmehl, J. Cohen, H. Plattner, Seventeen a-subunit isoforms of *Paramecium* V-ATPase provide high specialization in localization and function, Molecular Biology of the Cell 17 (2006) 917–930.

[19] M. Clarke, J. Kohler, Q. Arana, T. Liu, J. Heuser, G. Gerisch, Dynamics of the vacuolar H⁺-ATPase in the contractile vacuole complex and the endosomal pathway of *Dictyostelium* cells, Journal of Cell Science 115 (2002) 2893–2905.

[20] H.K. GrØnlien, C. Stock, M.S. Aihara, R.D. Allen, Y. Naitoh, Relationship between the membrane potential of the contractile vacuole complex and its osmoregulatory activity in *Paramecium multimicronucleatum*, Journal of Experimental Biology 205 (2002) 3261–3270.

[21] C. Stock, H.K. GrØnlien, R.D. Allen, The ionic composition of the contractile vacuole fluid of *Paramecium* mirrors ion transport across the plasma membrane, European Journal of Cell Biology 81 (2002) 505–515.

[22] C. Stock, H.K. GrØnlien, R.D. Allen, Y. Naitoh, Osmoregulation in *Paramecium*: in situ ion gradients permit water to cascade through the cytosol to the contractile vacuole, Journal of Cell Science 115 (2002) 2339–2348.

[23] J. Beisson, Preformed cell structure and cell heredity, Prion 2 (2008) 1–8.

[24] R.D. Allen, M.S. Ueno, A.K. Fok, A survey of lectin binding in *Paramecium*, Journal of Protozoology 35 (1988) 400–407.

[25] J.L. Browning, D.L. Nelson, Biochemical studies of the excitable membrane of *Paramecium aurelia*. I. $^{45}Ca^{2+}$ fluxes across resting and excited membrane, Biochimica et Biophysica Acta 448 (1976) 338–351.

[26] T. Shigaki, I. Rees, L. Nakhleh, K.D. Hirschi, Identification of three distinct phylogenetic groups of CAX cation/proton antiporters, Journal of Molecular Evolution 63 (2006) 815–825.

[27] E.K. Rooney, J.D. Gross, ATP-driven Ca^{2+}/H^+ antiport in acid vesicles from *Dictyostelium*, Proceedings of the National Academy of Sciences of the United States of America 89 (1992) 8025–8029.

[28] E.M. Ladenburger, I. Korn, N. Kasielke, T. Wassmer, H. Plattner, An Ins(1,4,5)P_3 receptor in *Paramecium* is associated with the osmoregulatory system, Journal of Cell Science 119 (2006) 3705–3717.

[29] E.M. Ladenburger, H. Plattner, Calcium-release channels in *Paramecium*. Genomic expansion, differential positioning and partial transcriptional elimination, PLoS ONE 6 (2011) e27111.

[30] T. Tominaga, Y. Naitoh, R.D. Allen, A key function of non-planar membranes and their associated microtubular ribbons in contractile vacuole membrane dynamics is revealed by electrophysiologically controlled fixation of *Paramecium*, Journal of Cell Science 112 (1999) 3733–3745.

[31] T. Tani, R.D. Allen, Y. Naitoh, Periodic tension development in the membrane of the in vitro contractile vacuole of *Paramecium multimicronucleatum*: modification by bisection, fusion and suction, Journal of Experimental Biology 203 (2000) 239–251.

[32] R. Kissmehl, I.M. Sehring, E. Wagner, H. Plattner, Immunolocalization of actin in *Paramecium* cells, Journal of Histochemistry and Cytochemistry 52 (2004) 1543–1559.

[33] I.M. Sehring, C. Reiner, J. Mansfeld, H. Plattner, R. Kissmehl, A broad spectrum of actin paralogs in *Paramecium tetraurelia* cells display differential localization and function, Journal of Cell Science 120 (2007) 177–190.

[34] R. Jahn, R.H. Scheller, SNAREs – engines for membrane fusion, Nature Reviews Molecular Cell Biology 7 (2006) 631–643.

[35] D. Fasshauer, R.B. Sutton, A.T. Brunger, R. Jahn, Conserved structural features of the synaptic fusion complex: SNARE proteins reclassified as Q- and R-SNAREs, Proceedings of the National Academy of Sciences of the United States of America 95 (1998) 15781–15786.

[36] S.W. Whiteheart, T. Schraw, E.A. Matveeva, N-ethylmaleimide sensitive factor (NSF) structure and function, International Review of Cytology 207 (2001) 71–112.

[37] R. Kissmehl, M. Froissard, H. Plattner, M. Momayezi, J. Cohen, NSF regulates membrane traffic along multiple pathways in *Paramecium*, Journal of Cell Science 115 (2002) 3935–3946.

[38] C. Schilde, T. Wassmer, J. Mansfeld, H. Plattner, R. Kissmehl, A multigene family encoding R-SNAREs in the ciliate *Paramecium tetraurelia*, Traffic 7 (2006) 440–455.

[39] C. Schilde, K. Lutter, R. Kissmehl, H. Plattner, Molecular identification of a SNAP-25-like SNARE protein in *Paramecium*, Eukaryotic Cell 7 (2008) 1387–1402.

[40] C. Schilde, B. Schonemann, I.M. Sehring, H. Plattner, Distinct subcellular localization of a group of synaptobrevin-like SNAREs in *Paramecium tetraurelia* and effects of silencing SNARE-specific chaperone NSF, Eukaryotic Cell 9 (2010) 288–305.

[41] R. Kissmehl, C. Schilde, T. Wassmer, C. Danzer, K. Nuehse, K. Lutter, H. Plattner, Molecular identification of 26 syntaxin genes and their assignment to the different trafficking pathways in *Paramecium*, Traffic 8 (2007) 523–542.

[42] H. Plattner, How to design a highly organized cell: an unexpectedly high number of widely diversified SNARE proteins positioned at strategic sites in the ciliate, *Paramecium tetraurelia*, Protist 161 (2010) 497–516.

[43] H. Plattner, Membrane trafficking in protozoa SNARE proteins, H⁺-ATPase, actin, and other key players in ciliates, International Review of Cell and Molecular Biology 280 (2010) 79–184.

[44] M. Zerial, H. McBride, Rab proteins as membrane organizers, Nature Reviews Molecular Cell Biology 2 (2001) 107–117.

[45] L.J. Bright, N. Kambesis, S.B. Nelson, B. Jeong, A.P. Turkewitz, Comprehensive analysis reveals dynamic and evolutionary plasticity of Rab GTPases and membrane traffic in *Tetrahymena thermophila*, PLoS Genetics 6 (2010) e1001155.

[46] A. Galvani, L. Sperling, RNA interference by feeding in *Paramecium*, Trends in Genetics 18 (2002) 11–12.

[47] T.M. Sonneborn, Methods in *Paramecium* research, in: D.M. Prescott (Ed.), Methods in Cell Physiology 4, Academic Press, Inc., London, 1970, pp. 242–335.

[48] J. Sambrook, E. Fritch, T. Maniatis (Eds.), Molecular Cloning: A Laboratory Manual, Cold Spring Harbor Laboratory Press, Cold Spring Harbor, NY, 1989.

[49] L. Timmons, D.L. Court, A. Fire, Ingestion of bacterially expressed dsRNAs can produce specific and potent genetic interference in *Caenorhabditis elegans*, Gene 263 (2001) 103–112.

[50] M. Iwamoto, R.D. Allen, Y. Naitoh, Hypo-osmotic or Ca^{2+}-rich external conditions trigger extra contractile vacuole complex generation in *Paramecium multimicronucleatum*, Journal of Experimental Biology 206 (2003) 4467–4473.

[51] T. Tominaga, R. Allen, Electrophysiology of the in situ contractile vacuole complex of *Paramecium* reveals its membrane dynamics and electrogenic site during osmoregulatory activity, Journal of Experimental Biology 201 (1998) 451–460.

[52] M. Ishida, A.K. Fok, M.S. Aihara, R.D. Allen, Hyperosmotic stress leads to reversible dissociation of the proton pump-bearing tubules from the contractile vacuole complex in *Paramecium*, Journal of Cell Science 109 (1996) 229–237.

[53] M. Miaczynska, H. Stenmark, Mechanisms and functions of endocytosis, Journal of Cell Biology 180 (2008) 7–11.

[54] M.L. Schwartz, A.J. Merz, Capture and release of partially zipped trans-SNARE complexes on intact organelles, Journal of Cell Biology 185 (2009) 535–549.

[55] C. Grefen, A. Honsbein, M.R. Blatt, Ion transport, membrane traffic and cellular volume control, Current Opinion in Plant Biology 14 (2011) 332–339.

[56] Y. Hagalili, N. Bachnoff, D. Atlas, The voltage-gated Ca^{2+} channel is the Ca^{2+} sensor protein of secretion, Biochemistry 47 (2008) 13822–13830.

[57] J.H. Schwartz, G. Li, Q. Yang, V. Suri, J.J. Ross, E.A. Alexander, Role of SNAREs and H⁺-ATPase in the targeting of proton pump-coated vesicles to collecting duct cell apical membrane, Kidney International 72 (2007) 1310–1315.

[58] V. Marshansky, M. Futai, The V-type H⁺-ATPase in vesicular trafficking: targeting, regulation and function, Current Opinion in Cell Biology 20 (2008) 415–426.

[59] J. Heuser, Evidence for recycling of contractile vacuole membrane during osmoregulation in *Dictyostelium* amoebae – a tribute to Günther Gerisch, European Journal of Cell Biology 85 (2006) 859–871.

[60] J. Bush, L. Temesvari, J. Rodriguez-Paris, G. Buczynski, J. Cardelli, A role for a Rab4-like GTPase in endocytosis and in regulation of contractile vacuole structure and function in *Dictyostelium discoideum*, Molecular Biology of the Cell 7 (1996) 1623–1638.

[61] Y. Saito-Nakano, T. Nakahara, K. Nakano, T. Nozaki, O. Numata, Marked amplification and diversification of products of ras genes from rat brain, Rab GTPases, in the ciliates *Tetrahymena thermophila* and *Paramecium tetraurelia*, Journal of Eukaryotic Microbiology 57 (2010) 389–399.

[62] K. Komsic-Buchmann, L.M. Stephan, B. Becker, The SEC6 protein is required for contractile vacuole function in *Chlamydomonas reinhardtii*, Journal of Cell Science 125 (2012) 2885–2895.

[63] M. Essid, N. Gopaldass, K. Yoshida, C. Merrifield, T. Soldati, Rab8a regulates the exocyst-mediated kiss-and-run discharge of the *Dictyostelium* contractile vacuole, Molecular Biology of the Cell 23 (2012) 1267–1282.

[64] H. Plattner, I.M. Sehring, I.K. Mohamed, K. Miranda, W. De Souza, R. Billington, A. Genazzani, E.M. Ladenburger, Calcium signaling in closely related protozoan groups (Alveolata): non-parasitic ciliates (*Paramecium*, *Tetrahymena*) vs. parasitic Apicomplexa (*Plasmodium*, *Toxoplasma*), Cell Calcium 51 (2012) 351–382.

[65] F. Wuytack, L. Raeymaekers, L. Missiaen, PMR1/SPCA Ca^{2+} pumps and the role of the Golgi apparatus as a Ca^{2+} store, Pflugers Archiv 446 (2003) 148–153.

[66] Y. Naitoh, T. Tominaga, M. Ishida, A. Fok, M. Aihara, R. Allen, How does the contractile vacuole of *Paramecium multimicronucleatum* expel fluid? Modelling the expulsion mechanism, Journal of Experimental Biology 200 (1997) 713–721.

[67] T. Tani, R.D. Allen, Y. Naitoh, Cellular membranes that undergo cyclic changes in tension: direct measurement of force generation by an in vitro contractile vacuole of *Paramecium multimicronucleatum*, Journal of Cell Science 114 (2001) 785–795.

[68] N. Mohandas, E. Evans, Mechanical properties of the red cell membrane in relation to molecular structure and genetic defects, Annual Review of Biophysics and Biomolecular Structure 23 (1994) 787–818.

[69] O.S. Andersen, R.E. Koeppe, Bilayer thickness and membrane protein function: an energetic perspective, Annual Review of Biophysics and Biomolecular Structure 36 (2007) 107–130.

[70] N. Groulx, F. Boudreault, S.N. Orlov, R. Grygorczyk, Membrane reserves and hypotonic cell swelling, Journal of Membrane Biology 214 (2006) 43–56.

[71] C.L. Brett, A.J. Merz, Osmotic regulation of Rab-mediated organelle docking, Current Biology 18 (2008) 1072–1077.

[72] M. Wu, B. Huang, M. Graham, A. Raimondi, J.E. Heuser, X. Zhuang, P. De Camilli, Coupling between clathrin-dependent endocytic budding and F-BAR-dependent tubulation in a cell-free system, Nature Cell Biology 12 (2010) 902–908.

[73] R.J. Heath, R.H. Insall, *Dictyostelium* MEGAPs: F-BAR domain proteins that regulate motility and membrane tubulation in contractile vacuoles, Journal of Cell Science 121 (2008) 1054–1064.

[74] E. Harris, K. Yoshida, J. Cardelli, J. Bush, Rab11-like GTPase associates with and regulates the structure and function of the contractile vacuole system in *Dictyostelium*, Journal of Cell Science 114 (2001) 3035–3045.

[75] A.H. Hutagalung, P.J. Novick, Role of Rab GTPases in membrane traffic and cell physiology, Physiological Reviews 91 (2011) 119–149.

[76] M. Ishida, M.S. Aihara, R.D. Allen, A.K. Fok, Osmoregulation in *Paramecium*: the locus of fluid segregation in the contractile vacuole complex, Journal of Cell Science 106 (1993) 693–702.

[77] J. Moniakis, M.B. Coukell, A. Janiec, Involvement of the Ca^{2+}-ATPase PAT1 and the contractile vacuole in calcium regulation in *Dictyostelium discoideum*, Journal of Cell Science 112 (1999) 405–414.

[78] Y. Xie, M.B. Coukell, Z. Gombos, Antisense RNA inhibition of the putative vacuolar H^+-ATPase proteolipid of *Dictyostelium* reduces intracellular Ca^{2+} transport and cell viability, Journal of Cell Science 109 (1996) 489–497.
[79] E.M. Ladenburger, I.M. Sehring, I. Korn, H. Plattner, Novel types of Ca^{2+} release channels participate in the secretory cycle of *Paramecium* cells, Molecular and Cellular Biology 29 (2009) 3605–3622.
[80] L. Lapatsina, J. Brand, K. Poole, O. Daumke, G.R. Lewin, Stomatin-domain proteins, European Journal of Cell Biology 91 (2012) 240–245.
[81] K. Fujiu, Y. Nakayama, H. Iida, M. Sokabe, K. Yoshimura, Mechanoreception in motile flagella of *Chlamydomonas*, Nature Cell Biology 13 (2011) 630–632.
[82] R. Xiao, X.Z. Xu, Mechanosensitive channels: in touch with Piezo, Current Biology 20 (2010) R936–R938.
[83] C. Kung, B. Martinac, S. Sukharev, Mechanosensitive channels in microbes, Annual Review of Microbiology 64 (2010) 313–329.
[84] E.K. Hoffmann, I.H. Lambert, S.F. Pedersen, Physiology of cell volume regulation in vertebrates, Physiological Reviews 89 (2009) 193–277.